J Physiol 588.8 (2010) pp 1227–1240

The Journal of Physiology

The calcium-permeable non-selective cation channel TRPM2 is modulated by cellular acidification

John G. Starkus[1,2], Andrea Fleig[2] and Reinhold Penner[2]

[1] *Pacific Biosciences Research Center, University of Hawaii, Honolulu, HI 96822, USA*
[2] *Laboratory of Cell and Molecular Signaling, Center for Biomedical Research at The Queen's Medical Center and John A. Burns School of Medicine at the University of Hawaii, Honolulu, HI 96813, USA*

TRPM2 is a calcium-permeable non-selective cation channel expressed in the plasma membrane and in lysosomes that is critically involved in aggravating reactive oxygen species (ROS)-induced inflammatory processes and has been implicated in cell death. TRPM2 is gated by ADP-ribose (ADPR) and modulated by physiological processes that produce peroxide, cyclic ADP-ribose (cADPR), nicotinamide adenine dinucleotide phosphate (NAADP) and Ca^{2+}. We investigated the role of extra- and intracellular acidification on heterologously expressed TRPM2 in HEK293 cells. Our results show that TRPM2 is inhibited by external acidification with an IC_{50} of pH 6.5 and is completely suppressed by internal pH of 6. Current inhibition requires channel opening and is strongly voltage dependent, being most effective at negative potentials. In addition, increased cytosolic pH buffering capacity or elevated $[Ca^{2+}]_i$ reduces the rate of current inactivation elicited by extracellular acidification, and Na^+ and Ca^{2+} influence the efficacy of proton-induced inactivation. Together, these results suggest that external protons permeate TRPM2 channels to gain access to an intracellular site that regulates channel activity. Consistent with this notion, single-channel measurements in HEK293 cells reveal that internal protons induce channel closure without affecting single-channel conductance, whereas external protons affect channel open probability as well as single-channel conductance of native TRPM2 in neutrophils. We conclude that protons compete with Na^+ and Ca^{2+} for channel permeation and channel closure results from a competitive antagonism of protons at an intracellular Ca^{2+} binding site.

(Resubmitted 15 January 2010; accepted after revision 25 February 2010; first published online 1 March 2010)
Corresponding author J. Starkus: University of Hawaii, Pacific Biosciences Research Center, Queens Medical Center, University Tower, 814, 1356 Lusitania Street, Honolulu Hi 96813, USA. Email: johns@pbrc.hawaii.edu

Abbreviations ADPR, ADP-ribose; ASIC, acid-sensing ion channel; nDVF, nominally divalent-free; NMDG, *N*-methyl-D-glucamine.

Introduction

Ion channels in the plasma membrane or intracellular compartments may experience significant changes in proton concentrations. For example, various organelles such as acidic vesicles and lysosomes can maintain physiological pH levels below 5 (Lange *et al.* 2009). Extracellular acidification has been associated with a number of pathophysiological conditions, including inflammation, neurodegeneration, ischaemia and cancer (Kellum *et al.* 2004; Fang *et al.* 2008; Isaev *et al.* 2008). Accumulation of extracellular protons can also promote tissue acidosis and pain sensation (McMahon & Jones, 2004; Naves & McCleskey, 2005).

Depending on the type, acidification can either activate or inhibit ion channels. For example, the capsaicin receptor transient receptor potential vanilloid 1 (TRPV1; Lambert & Oberwinkler, 2005; Pingle *et al.* 2007) and acid-sensing ion channels (ASICs; Xiong *et al.* 2008) are activated by extracellular acidification and implicated in sensory pain transduction (Jordt *et al.* 2000). Protons functionally enhance the magnesium-conducting TRP channel melastatin 7 (TRPM7) by influencing its selectivity to monovalents (Jiang *et al.* 2005), but exert inhibitory effects on TRPV5 (Vennekens *et al.* 2001) and TRPM5 (Liu *et al.* 2005), ion channels involved in epithelial calcium (Ca^{2+}) influx and taste sensation, respectively.

The aim of the present study was to elucidate the sensitivity of TRPM2 channels to extracellular and internal acidification, since this channel can be expressed in both the plasma membrane (Perraud *et al.* 2001) and in

DOI: 10.1113/jphysiol.2010.187476

lysosomes (Lange *et al.* 2009), both of which may expose this channel to acidic environments. Moreover, native TRPM2 is expressed in neutrophils and monocytes, which are cells that migrate to sites of inflammation where pH levels can be quite acidic.

TRPM2 is a member of the transient receptor potential (TRP) melastatin subfamily of ion channels (Perraud *et al.* 2001). It plays a key role in aggravating inflammatory processes (Yamamoto *et al.* 2008) and has been implicated in cell death (Hara *et al.* 2002). The TRPM2 protein has two distinct domains functioning as ion channel and ADP-ribose (ADPR)-specific pyrophosphatase, respectively (Perraud *et al.* 2001; Sano *et al.* 2001; Hara *et al.* 2002). The primary gating mechanism of TRPM2 is through the binding of ADPR (Perraud *et al.* 2001), but TRPM2 currents can also be activated by reactive oxygen species (ROS) (Hara *et al.* 2002) through ROS-induced ADPR-release from mitochondria (Perraud *et al.* 2005). In addition to ROS, TRPM2 is synergistically regulated by a multitude of signalling molecules, including cyclic ADP-ribose (cADPR) (Kolisek *et al.* 2005), nicotinic acid adenine dinucleotide phosphate (NAADP) (Beck *et al.* 2006) and intracellular Ca^{2+} (Perraud *et al.* 2001; McHugh *et al.* 2003; Starkus *et al.* 2007). So far, only AMP has been found to exert negative feedback regulation of TRPM2 (Kolisek *et al.* 2005). The present study now demonstrates that acidic pH represents a second inhibitory modulator that can effectively inactivate TRPM2 channels at pH values in the range of 5–7.

Methods

Cell culture

Tetracycline-inducible HEK293 human Flag-TRPM2-expressing cells (HEK293-TRPM2) were cultured at 37°C with 5% CO_2 in Dulbecco's modified Eagle's medium (DMEM) supplemented with 10% fetal bovine serum as described previously (Perraud *et al.* 2001). The medium was supplemented with blasticidin (5 μg ml^{-1}, Invitrogen) and zeocin (0.4 mg ml^{-1}, Invitrogen). For induction, cells were resuspended in medium containing 1 μg ml^{-1} tetracycline (Invitrogen) 5–10 h before experiments. Isolation and maintenance of human neutrophils from whole human blood was performed as described previously and in accordance with institutional regulations (Lange *et al.* 2008) and the *Declaration of Helsinki*.

Solutions

For patch-clamp experiments, cells were kept in either regular sodium-based solution containing (mM): 140 NaCl, 1 $CaCl_2$, 11 glucose, 10 HEPES-NaOH (pH 8.0, 300 mosmol l^{-1}); or *N*-methyl-D-glucamine-based solution containing (mM): 140 *N*-methyl-D-glucamine (NMDG)-Cl, 1 $CaCl_2$, 11 glucose, 10 HEPES-NMG (pH 8, 300 mosmol l^{-1}). The pH of the relevant external solution was adjusted to pH 8, 7, or 6 using either NMDG, NaOH or HCl. To maintain Na^+ and K^+ free conditions in NMDG solutions, pH adjustments were made only with NMDG (a strong base) and HCl. For pH 5 and 6, HEPES buffer was replaced with acetate and MES, respectively. Cells were superfused using the SmartSquirt delivery system (Auto-Mate Scientific, San Francisco CA, USA). This system included a ValveLink TTL interface between the electronic valves and the EPC9 amplifier (HEKA, Lambrecht, Germany). This configuration allowed for programmable solution changes via the PatchMaster software (HEKA, Lambrecht, Germany). Standard pipette-filling solutions (Kglut) contained (mM): 140 potassium glutamate, 8 NaCl, 1 $MgCl_2$, 10 HEPES-KOH (pH 7.2, 300 mosmol l^{-1}). $[Ca^{2+}]_i$ was buffered to 300, 500, 800 or 3000 nM with 10 mM BAPTA and 5.7, 6.9, 7.8 or 9.3 mM $CaCl_2$, respectively, calculated with WebMaxC and as indicated in the text. Standard internal $[Ca^{2+}]_i$ was 800 nM. TRPM2 currents were activated by adding 1 mM ADPR (Sigma) to the pipette solution, unless indicated otherwise. Internal pH adjustments to pH 6.5 or 6.0 were done using HCl and MES buffer.

Electrophysiology

Patch-clamp experiments were performed in the whole-cell configuration at 21–25°C. Patch pipettes had resistances of 2–3 MΩ for whole-cell and 3–5 MΩ for single-channel experiments. Data were acquired with PatchMaster software controlling an EPC-9 amplifier. Voltage ramps of 50 ms spanning the voltage range from −100 to +100 mV were delivered from a holding potential of 0 mV at a rate of 0.5 Hz, typically over a period of 100–300 s. Voltages were corrected for a liquid junction potential of 10 mV. Currents were filtered at 2.9 kHz and digitized at 100 μs intervals. Capacitive currents were determined and corrected before each voltage ramp. The low-resolution temporal development of currents for a given potential was extracted from individual ramp current records by measuring the current amplitudes at voltages of −80 mV and +80 mV. Data at +80 mV were chosen for display in figures. Data were analysed with FitMaster (HEKA, Lambrecht, Germany), and IgorPro (WaveMetrics, Lake Oswego, OR, USA). Where applicable, statistical errors of averaged data are given as means ± S.E.M. with n determinations. Single ramps were plotted as current–voltage (I–V) relationships.

Single-channel measurements

In HEK293-TRPM2 cells, single-channel recordings were performed on excised patches in the inside-out configuration. The excised patch was exposed to an internal caesium glutamate-based solution containing 1 mM ADPR, with calcium clamped to 800 nM (pH 7). To test for pH effects, the same solution, but adjusted to pH 6, was applied to patch. The pipette external solution contained (mM): 140 caesium glutamate, 8 NaCl, 1 $CaCl_2$, 10 HEPES-CsOH (pH 7.2, 300 mosmol l^{-1}). A voltage step protocol of 20 s length and to −80 mV was applied repetitively from a holding potential of 0 mV with 1 s long breaks in acquisition between individual voltage pulses. Data were acquired at 1 kHz and filtered at 30 Hz for display purposes. Currents were baseline subtracted and unitary current amplitudes were determined by fitting Gaussian functions to single channel events displayed as all-point histograms. Single-channel conductance at −80 mV was then estimated using Ohm's law.

In human neutrophils, single-channel recordings were performed in the whole-cell configuration using the regular Na^+-based external solution that contained 1 mM $CaCl_2$ (see above). Internal K^+ ions were replaced with Cs^+ while keeping other ions constant (see internal solution above) and Ca^{2+} was left unbuffered. TRPM2 currents were evoked by perfusing cells with 300 nM subthreshold ADPR (Lange *et al.* 2008). Data acquisition and analysis were the same as described for the inside-out configuration above.

Results

Extracellular acidity inactivates TRPM2 currents

To test for a possible regulatory effect of pH on TRPM2 activity, we exposed cells to extracellular changes in acidity. We performed whole-cell patch-clamp experiments using the tetracycline-inducible HEK293 system expressing human TRPM2 channels following exposure to 1 μM tetracycline for 5–10 h (Perraud *et al.* 2001). Cells were kept in either Na^+- or $NMDG^+$-based extracellular solutions containing 1 mM Ca^{2+} and pH adjusted to 8. This pH level was chosen as it yielded stable currents with minimal inactivation. After whole-cell break-in, cells were perfused with a potassium glutamate-based internal solution (see Methods), supplemented with 1 mM ADP-ribose (ADPR) and internal Ca^{2+} concentration clamped at 800 nM using an appropriate mixture of BAPTA and $CaCl_2$ (see Methods), with internal pH adjusted to 7.3. A standard voltage ramp ranging between −100 mV and +100 mV and of 50 ms length was applied at 0.5 Hz to record TRPM2 currents. The inward and outward currents were extracted at −80 mV and +80 mV, respectively, and plotted *versus* time.

Under the above conditions, with Na^+-based external solutions and pH 8, ADPR rapidly activated inward and outward currents (Fig. 1*A*, black trace), reaching maximum amplitude and steady-state level within 40 s. To help distinguish TRPM2 currents from leak currents, most experiments were carried out with external solutions in which Na^+ ions were replaced with the less permeating cation NMDG, which retained large outward currents, but largely suppressed inward currents (Fig. 1*A*, red trace). This also shifted the reversal potential of TRPM2 currents from 0 mV to −60 mV (Fig. 1*B*). Figure 1*C* illustrates a typical protocol for investigating acidic pH-induced inactivation of TRPM2 currents. Initially, pH was kept at pH 8 and ADPR activated all available channels within 40 s in either Na^+- or $NMDG^+$-based solutions. Following maximum activation of TRPM2, cells were superfused for 200 s with the same external solution adjusted to pH 6. This produced a slow rate of current decay in Na^+-based solution and a faster rate of current decay in $NMDG^+$-based solution. Following the low pH exposure, pH was switched back to pH 8, resulting in nearly complete recovery of currents. Figure 1*D* shows the current–voltage (*I–V*) relationships obtained at pH 6 with external Na^+ (black trace) or $NMDG^+$ (red trace) at 100 s into the experiment. At pH 6 with Na^+-based solutions, both inward and outward currents were reduced by half, whereas the reversal potential of the current was not affected and remained at 0 mV, indicating no change in the channel selectivity. However, comparing the *I–V* relationship for pH 6 (black trace) with that obtained at pH 8 (dashed line; scaled by a factor of 0.5 to match outward current amplitudes at pH 6) reveals a voltage-dependent block, with the currents being more strongly blocked at negative voltages. The overall reduction in current magnitude may reflect pH-induced inactivation of TRPM2 and the more pronounced block of inward current at negative voltages may reflect a permeation block of Na^+ current by protons.

To further assess proton permeation, we attempted to measure proton currents directly in the absence of Na^+ and Ca^{2+} ions, but this failed to unambiguously elicit significant proton currents at pH 5 in TRPM2-overexpresing cells compared to wild-type HEK293 cells. These experiments were complicated by the presence of contaminating currents through endogenous acid-sensing ion channels (ASICs) (Shimada *et al.* 2006; Xiong *et al.* 2008) and/or pH-induced chloride currents (Nobles *et al.* 2004; Lambert & Oberwinkler, 2005). Although these currents were small in the face of the large cation currents carried by TRPM2, they may mask small proton currents carried by TRPM2. Moreover, the very conditions to optimize proton currents (absence of permeant cations and acidic pH 5) also favour fast and complete closure of TRPM2. Finally, it is possible that protons cannot actually fully traverse the channel

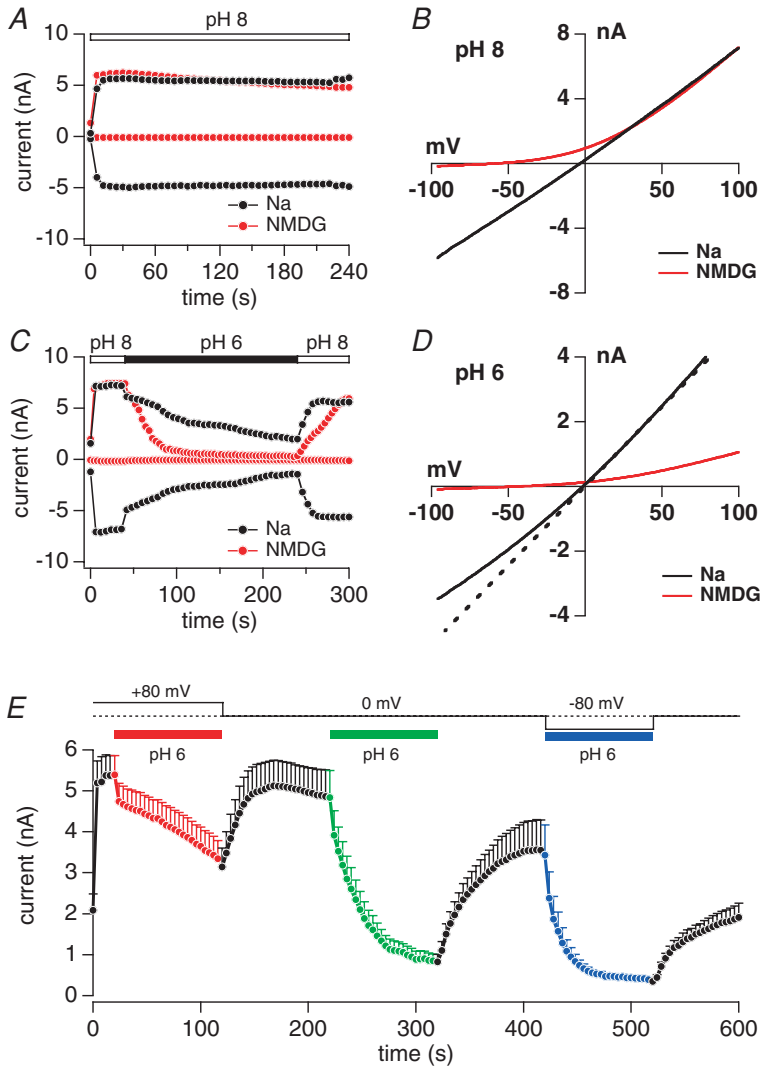

Figure 1. Extracellular acidification inactivates TRPM2 channels and inactivation rate is voltage dependent

A, examples of typical TRPM2 currents obtained from HEK293 cells inducibly overexpressing human TRPM2 (HEK293-TRPM2). Cells were kept at pH 8 in Na^+-based extracellular solution with 1 mM Ca^{2+} (black circles) and compared with $NMDG^+$-based solution with 1 mM Ca^{2+} (red circles). Internal solution was potassium glutamate based and buffered to 800 nM. It also contained 1 mM ADPR to maximally activate TRPM2 (see Methods). The voltage protocol consisted of 50 ms voltage ramps from −100 mV to +100 mV given at a frequency of 0.5 Hz. Data were extracted at −80 mV (inward current) and +80 mV (outward current). *B*, current–voltage (*I–V*) relationship of TRPM2 currents at pH 8 extracted at 100 s in Na^+- (black trace) or $NMDG^+$-based external solution (red trace). *C*, currents from example HEK293-TRPM2 cells kept in Na^+- (black trace) or $NMDG^+$-based (red trace) external solution. At the time indicated by the bar, external pH was lowered to pH 6. Same voltage protocol as in panel *A*. *D*, *I–V* curves extracted from the same cells as in *C* 100 s into the experiment and at pH 6 in external Na^+- (black) and $NMDG^+$-based solutions. The dashed line shows the *I–V* curve of TRPM2 current at 30 s into the experiment in Na^+-based solution at pH 8 but scaled by a factor of 0.5 to match the *I–V* curve at pH 6 (black line) at 100 s into the experiment. This comparison shows a voltage-dependent proton block at negative voltages. *E*, average TRPM2 currents ($n = 5$) extracted at +80 mV from HEK292-TRPM2 cells kept in $NMDG^+$-based solution supplemented with 1 mM Ca^{2+} and sequentially challenged with episodes of pH 6 at different holding potentials (V_{hold}) of +80 mV (red), 0 mV (green) and −80 mV (blue). Standard voltage ramps were delivered from the indicated holding potentials. The kinetics of inactivation at pH 6 were slowest at a holding potential of 80 mV and accelerated at 0 mV and −80 mV. At V_{hold} of +80 mV, current amplitudes remained above 50% for at least 100 s. At V_{hold} of 0 mV time for half-maximal inactivation $t_{1/2} = 24$ s and at −80 mV $t_{1/2} = 10$ s. During recovery periods from pH 6 (red, green and blue), pH was set to 8 and V_{hold} to 0 mV (black).

pore under these conditions, as proton permeation may require ionic interactions with Na^+ and/or Ca^{2+} to enable co-permeation. Such a phenomenon has been observed for example with Ba^{2+} permeation through CRAC channels, which cannot permeate when it is the only cation, but co-permeates with Na^+ when it is present (Lis *et al.* 2007).

The pH-induced change in rectification observed at negative voltages indicates that protons can affect ion transport across TRPM2 channels. This is consistent with the increased driving force for protons at negative voltages and would also predict a voltage-dependent change in the efficacy of pH-induced inactivation of TRPM2 currents. We assessed this in experiments where we exposed cells to the same extracellular pH 6, but at different holding potentials in between voltage ramps. All cells subjected to this protocol exhibited the same behaviour in that the pH-mediated inactivation was voltage dependent and accelerated at negative holding potentials (Fig. 1*E*). At +80 mV holding potential, inactivation was slow and incomplete within the time window of pH 6 exposure and presumably caused by the intermittent voltage ramps rather than the holding potential. Holding potentials of 0 mV and −80 mV exhibited progressively faster inactivation with half-maximal inhibition times of 24 s and 10 s, respectively. The voltage dependence of inactivation kinetics and degree of inhibition are consistent with the permeation of protons as they experience increased driving force at negative potentials.

Kinetics and magnitude of pH-induced inactivation

We next quantified the pH effect by activating TRPM2 currents at pH 8 under Na^+- or $NMDG^+$-based solutions and then exposing cells to various pH levels down to pH 5 (Fig. 2*A* and *C*, respectively). Increasing extracellular acidity progressively augmented and accelerated inactivation of TRPM2 with the strongest effect seen at pH 5, where outward currents were essentially abolished within a few seconds. Figure 2*B* illustrates the dose–response behaviour of TRPM2 current amplitudes at the end of the pH exposure as a function of proton concentration. Restoration of pH 8 at the end of pH episodes typically resulted in current recovery (Fig. 2*A* and *C*), except for pH 5, where the strong acidification was not reversible within 100 s. Current inactivation was biphasic and exhibited a prominent fast phase and a smaller slow component of current decline. While the magnitude and kinetics of the fast inactivation phase were pH dependent, the slower inactivation component did not appear to vary significantly with pH changes and is likely to represent channel rundown. Experiments performed with external $NMDG^+$-based solutions revealed that the pH-mediated inactivation was more pronounced (Fig. 2*B*) and significantly accelerated (Fig. 2*C*) compared to Na^+-based solutions. These data demonstrate that TRPM2 is inactivated by external acidification and that the presence of extracellular Na^+ partially protects TRPM2 from proton-induced inactivation, presumably by interfering with proton permeation.

The inactivation observed at pH 7 (Fig. 2*A* and *C*) indicates that TRPM2 channels are proton-sensitive near the physiological pH range and that some fraction of the channels will be inactivated even at physiological pH. To confirm this, we performed experiments where cells were exposed from 20 min to 1 h to $NMDG^+$ bath solutions with pH adjusted to 7 instead of pH 8. Under these conditions, whole-cell recordings showed a 20% current boost when pH 7 was shifted to pH 8 (see online Supplemental Material, Fig. S3*A*). This current boost was reduced when the bath pH of 8 was shifted to pH 9 (Fig. S3*B*). We hypothesize that this current boost most likely reflects channel recovery from inactivation caused by steady-state levels of protons.

Figure 2*D* illustrates the ionic requirements for recovery from pH-mediated inactivation, using external solutions containing either 1 mM Ca^{2+} or 1 mM Mg^{2+} or no divalents. Recovery occurred only in the presence of external Ca^{2+} and no recovery was observed with either Mg^{2+}- or divalent-free medium. In these recovery experiments, internal Ca^{2+} was buffered at 800 nM, suggesting that recovery is dependent on external Ca^{2+}. It is interesting to note that activation of TRPM2 can occur with nominally divalent-free external medium at normal pH (Starkus *et al.* 2007), but recovery from inactivation after prior acidification depends on the presence of external Ca^{2+}. This would suggest that the conformational state of pH-inactivated channels is distinct from the closed resting state and alters the Ca^{2+} requirements for re-opening.

The pH-mediated effects described above were entirely attributable to changes in proton concentration and not to pharmacological effects of the pH buffers, since control experiments with equimolar HEPES, MES and acetate at pH 8 had no significant effect on TRPM2 currents and inhibition of TRPM2 by pH 6 buffered with either MES or acetate were indistinguishable from each other (Fig. S1). HEK293 cells have been reported to express pH-induced chloride currents at pH values in the range of pH 4 to 5.5 (Nobles *et al.* 2004; Lambert & Oberwinkler, 2005). However, control experiments in which ADPR was excluded from the pipette solution, revealed only a very small increase in outward current of less than 50 pA at +80 mV in TRPM2-expressing HEK293 cells exposed to pH 5 (Fig. S2*A*), which is negligible in the face of typically several nanoamps of ADPR-induced outward currents that were essentially completely abolished by a shift to pH 5 (Fig. S2*B*). Given the variability of the reported chloride current magnitudes (Lambert & Oberwinkler, 2005) and the fact that our stable HEK293 cells were derived from

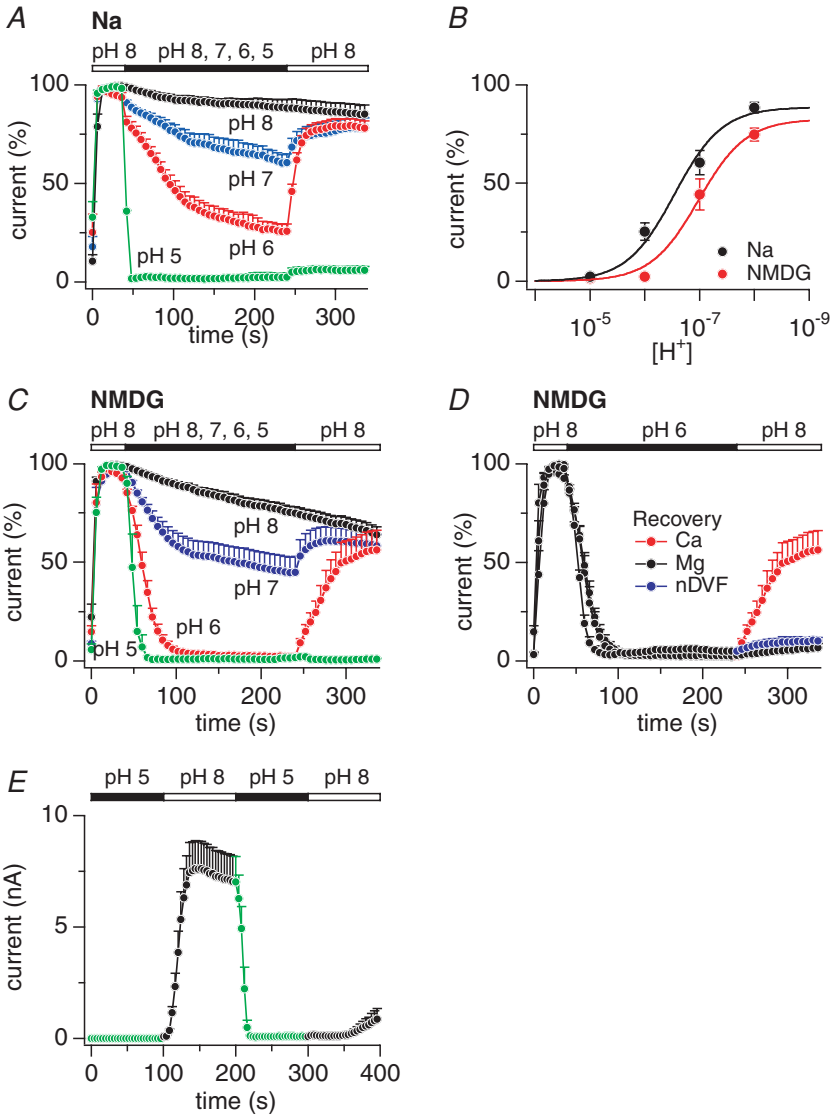

Figure 2. Extracellular acidification accelerates TRPM2 inactivation and recovery requires extracellular Ca^{2+}

A, normalized average currents in HEK293-TRPM2 cells kept in external Na^+ with 1 mM Ca^{2+} and exposed to decreasing pH. Currents evoked by 1 mM ADPR and 800 nM Ca^{2+} were assessed at +80 mV, normalized to the current amplitude at 38 s before application of different pH levels, then averaged and plotted *versus* time. Extracellular changes in pH were: pH 8 (black, $n = 4$), pH 7 (blue, $n = 9$), pH 6 (red, $n = 8$), pH 5 (green, $n = 6$). Data acquisition was as in Fig. 1*A*. Error bars represent S.E.M. *B*, dose–response behaviour of TRPM2 as a function of proton concentration measured at the end of external pH changes in Na^+- (black, $IC_{50} = 6.5$; Hill coefficient = 1) or $NMDG^+$-based solution (red; $IC_{50} = 7$; Hill coefficient = 1). *C*, normalized average TRPM2 currents extracted at +80 mV in $NMDG^+$-based solution supplemented with 1 mM Ca^{2+} and exposed to decreasing pH. Extracellular changes in pH were: pH 8 (black, $n = 8$), pH 7 (blue, $n = 11$), pH 6 (red, $n = 9$), pH 5 (green, $n = 5$). *D*, recovery of TRPM2 currents from acidification at pH 8 in $NMDG^+$-based external solution containing either 1 mM Ca^{2+} (red, $n = 9$), 1 mM Mg^{2+} (black, $n = 3$) or kept nominally divalent-free (blue, $n = 4$). *E*, average TRPM2 currents ($n = 9$) extracted at +80 mV in $NMDG^+$-based solution supplemented with 1 mM Ca^{2+}. Intact cells in the cell-attached configuration were exposed to 100 s of pH 5. At 100 s, whole-cell configuration was established and extracellular pH was returned to pH 8. At 200 s, cells with fully activated currents were again exposed to pH 5 to block open TRPM2 channels. At 300 s, pH 8 was re-established to demonstrate persistent block of open channels for at least 100 s. Note that with 100 s exposure times to pH 5 (in contrast to the 200 s exposure times in panels *A* and *C*), 2 of the 9 cells showed partial recovery from inactivation.

a single-cell clone expressing TRPM2, we surmise that this particular clonal line has no significant pH-induced chloride currents interfering with our TRPM2 currents. Furthermore, most acidification experiments in this study were carried out at pH 6, where such chloride currents are not normally activated.

While the change in *I–V* rectification at negative voltages and the pronounced effects of holding potential on kinetics and degree of inactivation support the notion that protons can permeate TRPM2 channels (Fig. 1*D* and *E*), the poorly irreversible inhibition of TRPM2 by pH 5 enabled us to address the question whether protons require channel opening to cause TRPM2 inactivation. To test this, we first exposed intact cells in the cell-attached configuration to pH 5 for 100 s and then activated TRPM2 by establishing the whole-cell configuration and concomitantly switching the extracellular solution to pH 8. If the pH effect were extracellular and closed TRPM2 channels were susceptible to pH 5-induced inactivation, one would expect ADPR to be ineffective in activating TRPM2 channels. However, as can be seen in Fig. 2*E*, the pH 5 exposure had no significant inhibitory effect on the subsequent activation of TRPM2 currents at pH 8 other than a slightly slower activation, which may have been caused by slight intracellular acidification of the cytosol while cells were exposed to pH 5 for 100 s. After TRPM2 currents had fully activated, a second application of pH 5 caused an immediate and complete block of TRPM2 currents that was poorly reversible within 100 s by returning to pH 8 in 7 out of 9 cells (7 cells did not recover at all within 100 s and 2 cells showed a delayed partial recovery). These results demonstrate that pH-mediated inactivation of TRPM2 requires the opening of channels and provide compelling evidence that the primary proton binding site responsible for channel inhibition is located intracellularly, distal to the channel's gate.

Effects of extracellular Ca^{2+} on pH-induced inactivation

Figure 3 illustrates the effects of extracellular Ca^{2+} on TRPM2 inactivation at different extracellular pH levels. First the channels were maximally activated using potassium glutamate-based internal solutions containing 1 mM ADPR and $[Ca^{2+}]_i$ buffered to 800 nM, while external solutions were kept at pH 8. Currents reached a steady-state level within 40 s and were normalized to maximum current. In experiments illustrated in Fig. 3*A*, pH remained at the level of pH 8 throughout the experiment, but external Ca^{2+} was decreased from 1 mM to 0.3 mM and nominally divalent-free (nDVF). Reducing extracellular Ca^{2+} to 0.3 mM had no effect on TRPM2 currents, which proceeded to decrease at a slow rate that was indistinguishable from that observed with 1 mM Ca^{2+} and was likely to be due to channel rundown. With nDVF, TRPM2 currents inactivated more rapidly, but recovered rapidly after readmission of 1 mM Ca^{2+}. When extracellular pH was drecreased to 7 in the presence of 1 mM extracellular Ca^{2+} (Fig. 3*B*), it caused pH-dependent inactivation of currents by about 50%. Reducing external Ca^{2+} to 0.3 mM or nominally zero (nDVF) augmented the extent of current inactivation and this effect was reversible upon restoring 1 mM Ca^{2+}. Conversely, increasing external Ca^{2+} to 3 mM during application of pH 7 significantly decreased the degree of current inactivation. Note that at different Ca^{2+} levels the current decrease exhibits fast and slow kinetic components. The faster rate of channel closure can be attributed to an increase in acidity from pH 8 to pH 7, whereas the slow rate is largely independent of pH or Ca^{2+} and likely to be caused by channel rundown. Finally, we exposed cells to pH 6, which resulted in rapid and complete inactivation of TRPM2 currents (Fig. 3*C*) and was not further augmented by a reduction in external Ca^{2+} to 0.3 mM or zero (nDVF). However, as in the case of pH 7, raising external Ca^{2+} to 3 mM effectively suppressed the pH-induced inactivation. These results suggest that protons and external Ca^{2+} may compete for a common binding site that requires Ca^{2+} to maintain channels in their open state.

Intracellular Ca^{2+} affects pH-induced inactivation

The above experiments investigated changes in extracellular Ca^{2+} concentration at fixed levels of $[Ca^{2+}]_i$. However, since TRPM2 is permeable to Ca^{2+} and channel activity is regulated by intracellular Ca^{2+} (Starkus *et al.* 2007; Csanady & Torocsik, 2009), the site (or sites) of action of Ca^{2+} are likely to be inside the pore or intracellular (see Fig. 2*D*). Cytosolic Ca^{2+} levels below 300 nM strongly accelerate inactivation of TRPM2 independently of extracelluar Ca^{2+} ions (Starkus *et al.* 2007). This mechanism seems to be mediated at least in part by the Ca^{2+}-sensitive modulator calmodulin (Tong *et al.* 2006; Starkus *et al.* 2007). We assessed whether internal Ca^{2+} affected the inactivation of TRPM2 currents induced by external acidification. HEK293-TRPM2 cells were exposed to extracellular pH 6 in $NMDG^+$ plus 1 mM Ca^{2+} and intracellularly perfused with increasing concentrations of $[Ca^{2+}]_i$ (Fig. 3*D*). We determined the individual pH-induced time constants of inactivation (τ) of each data trace acquired in Fig. 3*D* and found that inactivation was fastest at low intracellular Ca^{2+} and slowed down progressively at higher concentrations: 100 nM ($\tau = 3\text{ s} \pm 0.8$ s, $n = 10$), 300 nM ($\tau = 9 \pm 1.2$, $n = 7$), 500 nM ($\tau = 12\text{ s} \pm 1.9$ s, $n = 8$) and 800 nM ($\tau = 20\text{ s} \pm 3.6$ s, $n = 7$). These data indicate that externally applied protons compete with intracellular Ca^{2+} for a site that is involved in maintaining channel activity,

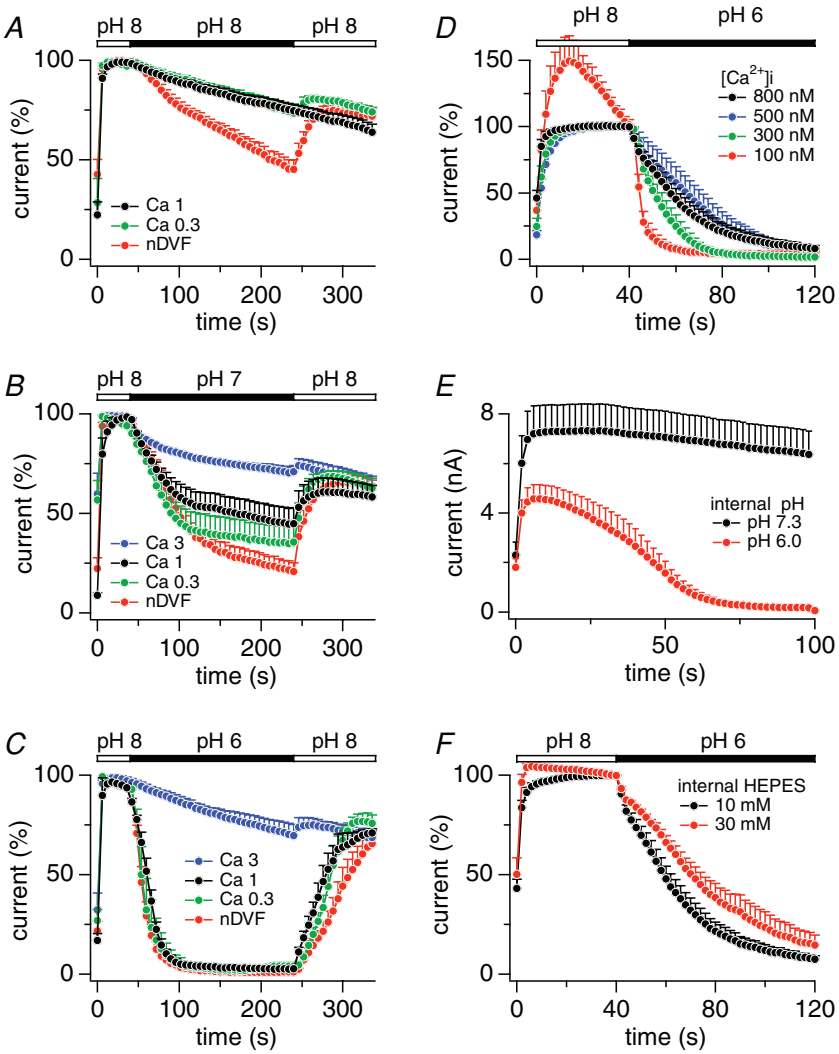

Figure 3. Intracellular acidification inactivates TRPM2 and extra- and intracellular Ca^{2+} counteract pH-induced inactivation

A, normalized average currents in HEK293-TRPM2 cells kept in $NMDG^+$-based solution with 1 mM Ca^{2+} and at pH 8. At the time indicated by the bar, external Ca^{2+} concentrations were kept at 1 mM Ca^{2+} (black circles, $n = 8$), reduced to 0.3 mM Ca^{2+} (green circles, $n = 4$) or reduced to nominally Ca^{2+}-free (red circles, $n = 5$). Data acquisition and analysis as in Fig. 2*A*. Error bars represent S.E.M. *B*, normalized average currents in HEK293-TRPM2 cells kept in $NMDG^+$-based solution with 1 mM Ca^{2+} and at pH 8. At the time indicated by the bar, external pH was reduced to pH 7 while Ca^{2+} concentration was set to 3 mM (blue, $n = 5$), 1 mM (black, $n = 11$), 0.3 mM (green, $n = 5$), or nominally divalent free (nDVF; red, $n = 6$). Error bars represent S.E.M. *C*, normalized average currents in HEK293-TRPM2 cells kept in $NMDG^+$-based solution with 1 mM Ca^{2+} and at pH 8. At the time indicated by the bar, external pH was reduced to pH 6 while Ca^{2+} concentration was set to 3 mM (blue, $n = 4$), 1 mM (black, $n = 7$), 0.3 mM (green, $n = 4$) or nDVF (red, $n = 6$). Error bars represent S.E.M. *D*, normalized average currents in HEK293-TRPM2 cells kept in $NMDG^+$-based solution with 1 mM Ca^{2+} and at pH 8. At the time indicated by the bar, external pH was reduced to pH 6 as indicated by the bar. Cells were perfused internally with K^+-based glutamate solution supplemented with 1 mM ADPR and various buffered Ca^{2+} concentrations of 100 nM (red closed circles, $n = 10$), 300 nM (green closed circles, $n = 7$), 500 nM (blue filled circles $n = 8$), or 800 nM (black closed circles, $n = 7$). Error bars represent S.E.M. *E*, average TRPM2 currents in HEK293-TRPM2 cells kept in $NMDG^+$-based solution with 1 mM Ca^{2+} and at pH 8. Cells were perfused with standard intracellular potassium glutamate solution supplemented with 1 mM ADPR and 800 nM $[Ca^{2+}]_i$ at pH 7.3 (black circles, $n = 11$) or pH 6 (red circles, $n = 11$). Error bars represent S.E.M. *F*, normalized average currents in HEK293-TRPM2 cells kept in $NMDG^+$-based solution with 1 mM Ca^{2+} and at pH 8. At the time indicated by the bar, external pH was reduced to pH 6 as indicated by the bar. Intracellular solution was standard potassium glutamate based solution supplemented with 1 mM ADPR and 800 nM $[Ca^{2+}]_i$ in the presence of either 10 mM HEPES (black, $n = 10$) or 30 mM HEPES (red, $n = 6$). Data were normalized by setting the current amplitude before application of pH 6 (48 s) as 100%.

consistent with proton permeation through TRPM2 channels and an intracellular site of action.

Intracellular pH affects TRPM2 currents

We next explored whether intracellular acidification at fixed extracellular pH of 8 could affect current inactivation. HEK293-TRPM2 cells were kept in $NMDG^+$ with 1 mM Ca^{2+} and perfused intracellularly with standard potassium glutamate-based solution containing 1 mM ADPR, 800 nM $[Ca^{2+}]_i$ and pH adjusted to either 7.3 (control) or 6. Figure 3*E* illustrates that increasing intracellular acidity to pH 6 strongly suppressed current activation and channels inactivated within 60 s after whole-cell establishment. Thus, intracellular protons can affect TRPM2 currents, indicating that the site (or sites) at which Ca^{2+} and protons interact are accessible to both modulators from either side of the membrane.

If external protons can gain access to this presumed intracellular site via permeation through open channels, one might expect that increasing intracellular buffering capacity for protons would reduce the efficacy of protons to inactivate TRPM2. Indeed, as shown in Fig. 3*F*, buffering intracellular pH to 7.3 with 30 mM HEPES slowed the kinetics of inactivation evoked by extracellular acidification to pH 6 in comparison to the same pH challenge with a HEPES concentration of 10 mM. The fact that HEPES was not able to prevent inactivation entirely suggests that the relevant site might be in a restricted space with limited access for Ca^{2+} and pH buffers, consistent with a prior report that suggested the Ca^{2+} binding site that regulates TRPM2 activity to be located in a deep crevice of the intracellular side of the protein (Csanady & Torocsik, 2009).

Protons elicit single-channel inactivation of heterologous and native TRPM2

In order to determine how intracellular protons affect single-channel behaviour, we conducted experiments in membrane patches excised from HEK293-TRPM2 cells using the inside-out configuration of the patch-clamp technique. Figure 4*A* shows consecutive currents obtained at –80 mV in two excised patches (upper and lower panel) representative of five experiments. The cytosolic side of the patch was exposed to standard internal solution with Cs^+ replacing K^+ and additionally containing 1 mM ADPR, with $[Ca^{2+}]_i$ clamped to 800 nM. The patch pipette contained caesium glutamate-based solution with 1 mM Ca^{2+} as the only divalent ion. After 20 s at pH 7, the cytosolic side was exposed to an identical solution with acidity adjusted to pH 6. This induced a fast and complete cessation of all channel activity within 5 s. Gaussian functions were fitted to the single channel events in the corresponding all-point histogram of Fig. 4*B*, revealing discrete peaks corresponding to unitary events of −5.1 pA

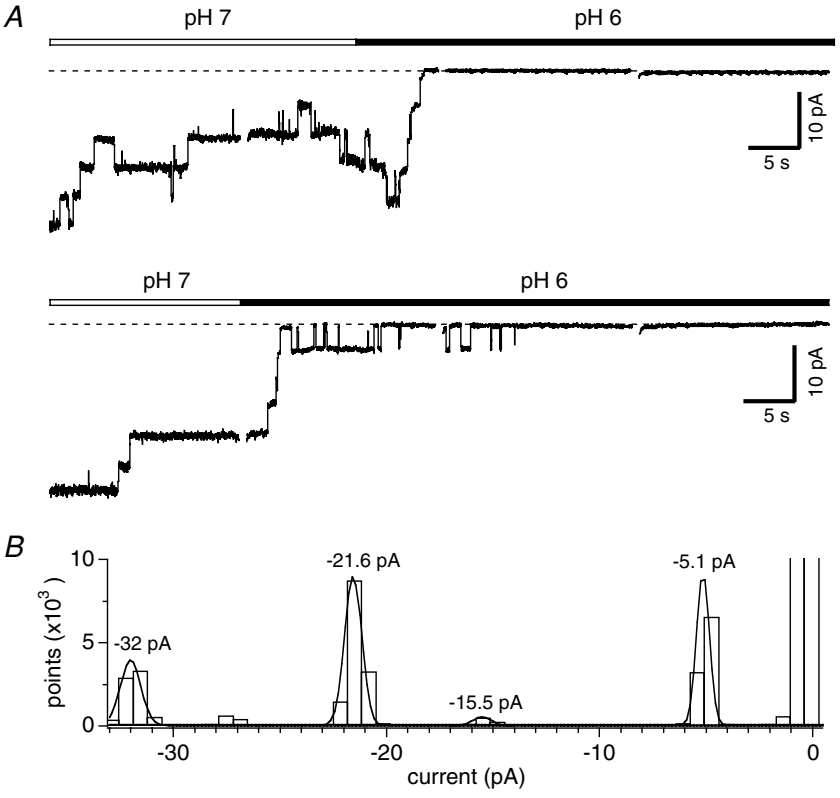

Figure 4. Intracellular pH induces channel closure of TRPM2 in membrane patches
A, representative single-channel current recordings of two inside-out patches pulled from HEK293-TRPM2 cells at −80 mV (upper and lower panels). TRPM2 was activated with 1 mM ADPR. Four consecutive traces are shown per inside out patch during the switch from pH 7 (open bar) to pH 6 (filled bar). Individual traces are 20 s long. Gaps between traces indicate a 1 s break (not to scale). A total of 4 additional patches showed similar results. *B*, all-point histogram of single-channel data shown in lower panel *A*. Data were fitted with Gaussian functions to estimate the single-channel current for 1, 3, 4 and 6 coinciding channel openings.

at −80 mV, equivalent to a single-channel conductance of 64 pS. This suggests that internal proton-induced current block was due to channel closure rather than a change in single channel conductance.

While heterologously expressed TRPM2 channels exhibit essentially the same properties as native channels with respect to mode of activation, there are some differences in sensitivity to the various modulators of channel activity, including IC_{50} values for ADPR and efficacy of modulation by Ca^{2+} and cADPR as well as single-channel conductance (Beck *et al.* 2006; Lange *et al.* 2008). Acidification has been reported to enhance neutrophil activation, delay cellular apoptosis, and negatively affect neutrophil migration (Lardner, 2001). We investigated whether native TRPM2 was pH sensitive in neutrophils isolated from human whole blood using the whole-cell configuration of the patch-clamp technique to record single-channel activity (Lange *et al.* 2008). The external solution was standard Na^+-based saline and intracellular K^+ ions were replaced with Cs^+ while Ca^{2+} was left unbuffered. The internal solution was additionally supplemented with subthreshold ADPR (300 nM). Upon whole-cell break-in, cells were kept at a holding potential of 0 mV and stimulated with consecutive 20 s voltage pulses to −80 mV at 1 s intervals. Once channel activity was observed, cells were superfused with external solution at pH 5 (Fig. 5*A*, representative cell out of a total of 6 experiments). This induced channel flickering and subsequent closure within 40 s. Note that after returning to pH 7, at least two channels resumed activity, demonstrating that inactivation was mediated by acidification in a reversible manner and not caused by simple rundown of channel activity. The all-point histogram of single-channel events during exposure to pH 7 (time 0 s to 70 s in Fig. 5*A*) revealed a single channel current of −3.4 pA when fitted with a Gaussian curve (Fig. 5*B*). This changed to −2.1 pA during the increase of extracellular acidity to pH 5 as assessed at time 86 s to 115 s (Fig. 5*C*). When averaging the single-channel currents obtained from all-point histograms and Gaussian fits of a total of six cells, the average single-channel current at pH 7 and −80 mV was -3.5 ± 0.06 pA compared to -2.3 ± 0.08 pA at pH 5 ($n = 6$). This corresponds to a single-channel conductance of 44 pS for pH 7 and 29 pS for pH 5. These data indicate that the reduction in native TRPM2 activity by external acidification is more complex than that of direct internal acidification (Fig. 4), as it is due to a combination of reduced open probability, channel closure, and a slight reduction in single-channel conductance.

Discussion

The present study provides evidence that ADPR-induced TRPM2 currents are sensitive to proton-induced regulation. We demonstrate that acidification of either the extra- or intracellular milieu can rapidly and potently inactivate TRPM2 currents. The increased proton concentration during an extracellular pH challenge induced inactivation of TRPM2 with an IC_{50} of pH 6.5 in Na^+-based Ringer solution and an IC_{50} of pH 6.9 in $NMDG^+$-based Ringer solution (Fig. 2*B*). Intracellular exposure to pH 6 was also effective and completely

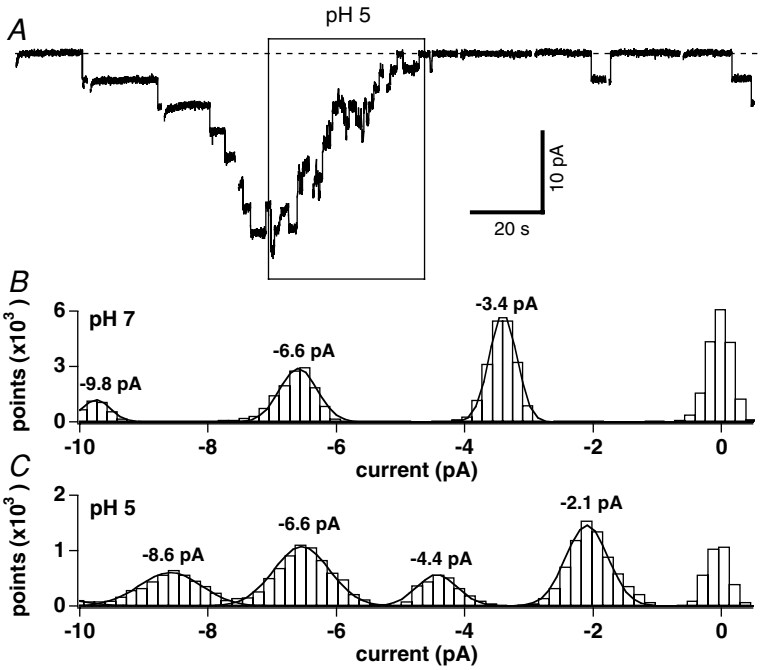

Figure 5. Extracellular acidification inactivates endogenous TRPM2 and reduces single channel conductance in human neutrophils
A, example data traces of TRPM2 single-channel events evoked by a low concentration of 300 nM ADPR in the whole-cell mode and measured in a representative neutrophil at −80 mV. Cells were kept in standard extracellular solution at pH 7 (see methods). pH 5 was applied during the time indicated by the box. Ten consecutive traces are shown. Individual traces are 20 s long. Gaps between traces indicate a 1 s break in data acquisition. A total of 5 additional cells showed similar results. *B*, all-point histogram of single channel events measured at pH 7 and extracted between 0 s and 70 s from data shown in panel *A*. Data were fitted with Gaussian functions to estimate the single-channel current. *C*, all-point histogram of single-channel events measured at pH 5 and extracted between 86 s and 115 s from data shown in panel *A*. Data were fitted with Gaussian functions to estimate the single channel current.

inactivated TRPM2 currents (Fig. 3*E*). Our results indicate that protons can access the TRPM2 channel pore just like Ca^{2+} and Na^{+}, since both ions affect pH-induced inactivation of TRPM2 (Fig. 1*C* and Fig. 3*A*–*C*). In addition, the current–voltage relationship revealed that increased extracellular acidity slightly reduced the Na^{+} currents at negative voltages (Fig. 1*D*), indicating permeation block of Na^{+} flux by protons. Consistent with this notion, whole-cell recordings revealed a strong voltage dependence of pH-induced inactivation that was enhanced at negative voltages where driving force for protons is largest (Fig. 1*E*). Furthermore, pH-dependent inactivation of TRPM2 by extracellular acidification was dependent on opening of channels (Fig. 2*E*), placing the proton interaction site distal to the channel gate at an intracellular location. Also consistent with proton permeation, single-channel recordings of endogenous TRPM2 in human neutrophils revealed a reduction of both open probability and channel conductance when exposing cells to increased extracellular acidity (Fig. 4), whereas cytosolic acidification resulted in simple channel closure in HEK293 cells (Figs 3*E* and 5). Together, these results suggest an intracellular site for protons on TRPM2, which is accessible from the extracellular and intracellular side of the channel. This site may be inside a deep crevice of the TRPM2 protein with limited access for Ca^{2+} and pH buffers (Fig. 3*D* and *F*) (Csanady & Torocsik, 2009). Since both ADPR and Ca^{2+} are required to sustain TRPM2 activity, it seems likely that protons may compete for Ca^{2+}, and proton-induced unbinding of Ca^{2+} would then result in channel closure. This would also explain why increasing Ca^{2+} concentrations extra- or intracellularly are able to counteract the inhibitory action of low pH (Fig. 3*A*–*C* and *D*, respectively).

After completion of this work and while this report was under review, a study by Du *et al.* reported similar inhibitory effects of pH on TRPM2 (Du *et al.* 2009). Both studies find that extracellular and intracellular pH can inhibit TRPM2 currents and there is also agreement that external pH affects single-channel conductance, whereas internal pH does not. There are, however, significant differences in the conclusions reached by the two studies. The potency of pH appears to be different, since for extracellular pH, Du *et al.* reported an IC_{50} of pH 5.3, whereas we find an IC_{50} of 6.5. One possible explanation for this discrepancy could be that Du *et al.* used 2 mM extracellular Ca^{2+}, whereas we used 1 mM. Since we demonstrate that increasing extracellular Ca^{2+} counteracts the pH-induced inhibition (Fig. 3), this could account for the reduced efficacy of pH reported by Du *et al.* The most significant contrast between the two studies, however, relates to the mechanism of action of protons. Du *et al.* concluded that extracellular protons do not permeate TRPM2 and therefore postulated two independent sites of action of protons located extra- and intracellularly, respectively. Our study, however, presents clear evidence for proton permeation and therefore can explain all pH effects by a simpler model where extracellular and intracellular protons have access to the same binding site at the intracellular side of the protein, likely to be by competing at a Ca^{2+} binding that is similarly accessible by extra- and intracellular Ca^{2+} (Starkus *et al.* 2007; Csanady & Torocsik, 2009). Du *et al.* based their conclusion that TRPM2 is not permeable to protons on four principal experimental observations: (1) actual proton currents could not be detected in whole-cell experiments, (2) IC_{50} values for external pH were not voltage dependent since holding potentials of −100 mV were no different from those at 0 mV despite the larger driving force, (3) extracellular NH_4Cl (through intracellular alkalinization) did not reverse the block caused by extracellular pH 4, and (4) intracellular Ca^{2+} had no effect on extracellular pH-mediated inhibition.

However, none of these observations are necessarily incompatible with proton permeation or access of protons to an intracellular site. (1) The absence of significant proton currents, which is seen in both studies, applies only to experimental conditions in which other permeant cations such as Na^{+} and Ca^{2+} are absent. As our data demonstrate, both Na^{+} and Ca^{2+} ions will affect the efficacy of protons to inactivate TRPM2, indicating that protons and Na^{+}/Ca^{2+} in fact do co-permeate. A similar co-permeation phenomenon is observed in CRAC channels, which are impermeant to Ba^{2+} in the absence of Na^{+}, but both ions will co-permeate when Na^{+} is present (Lis *et al.* 2007). (2) The similar IC_{50} values for pH-dependent inhibition of TRPM2 at holding potentials of 0 mV and −100 mV reported by Du *et al.* do not exclude voltage-dependent effects of permeating protons, since both voltages are below the reversal potential of protons under acidic conditions and still provide driving force for protons. Our data clearly demonstrate voltage dependence of instantaneous current–voltage relationships, with inward currents being inhibited by protons (see Fig. 1*D*). Moreover, we observe clear voltage dependence in the kinetics and efficacy of pH-mediated inhibition of TRPM2 at different holding potentials (see Fig. 1*E*). Importantly, at a more positive holding potential of +80 mV that is beyond the reversal potential for protons, pH-mediated inactivation is not only slowed, but also significantly reduced in magnitude. (3) The poor reversibility of extreme pH-induced inhibition cannot answer the question of whether the proton effect is extracellular or intracellular, since alkalinization is ineffective at reversing the inhibition at either side of the membrane. However, the poorly reversible inhibition by extreme acidic pH enabled us to demonstrate that protons cannot affect closed channels through an extracellular site, but require channel gating (Fig. 2*E*). This places the proton-mediated inhibition of TRPM2 beyond the

channel's gate at an intracellular site. (4) The fact that changes in intracellular Ca^{2+} do not significantly change the IC_{50} of extracellular pH-induced inhibition only applies to steady-state inhibition. However, intracellular Ca^{2+} clearly affects the kinetics of external pH inhibition (see Fig. 4). The reason why steady-state amplitudes are not affected by $[Ca^{2+}]_i$ is likely to be because this site appears to be localized within a limited diffusion space in a deep crevice of the intracellular mouth of the channel (Csanady & Torocsik, 2009). It is therefore not surprising that the limited diffusion will eventually cause a steady-state block. For the same reason, intracellular pH buffers can only affect the kinetics of the pH effect and not the steady state (see Fig. 5*B*).

The study by Du *et al.* also demonstrated that several extracellular and intracellular residues of the TRPM2 channel protein could affect pH-mediated inhibition when mutated. However, one needs to be very cautious in interpreting these mutations, since all of them, regardless of location, affect single-channel conductance and/or *I–V* behaviour. Any change in permeation or selectivity may affect Na^+, Ca^{2+} and H^+ fluxes. Without selectivity analysis, it remains speculative whether any of these mutations identify a proton binding site. As we show in Figs 2 and 3, there is no need for mutations to change the efficacy of protons to inhibit TRPM2. It suffices to alter the Na^+ or Ca^{2+} concentrations to do so.

Protons are involved in the regulation of several members of the TRP ion channel families. While TRPM2 is inactivated by cellular acidification (Fig. 2*A* and *C*), the gating of the capsaicin receptor TRPV1 is facilitated at decreased pH, whereby pH-sensitivity is conferred through a glutamine residue located just before the putative pore-forming region of the channel (Jordt *et al.* 2000). Here, it is thought that protons cause an increase in open probability rather than acting on the gating mechanism or changing unitary conductance. On the other hand, both TRPM6 and TRPM7, members of the melastatin subfamily of TRP channels, show strongly enhanced inward rectification upon extracellular acidification. This has been linked to a proton-induced unbinding of Ca^{2+} block. Two key residues in the putative pore region confer pH sensitivity in addition to Ca^{2+} and Mg^{2+} selectivity (Jiang *et al.* 2005; Li *et al.* 2007).

Proton-induced inhibition is observed in the Ca^{2+}-activated cation channel TRPM5 (Liu *et al.* 2005). This seems to be due to key residues located in extracellular domains with intracellular acidification having no effect on TRPM5 currents. TRPM2, on the other hand, is sensitive to both extracellular and intracellular acidification (Fig. 2*A* and *C* and Fig. 3*E*), which is also observed for the TRPV5 Ca^{2+} channel (Vennekens *et al.* 2001; Yeh *et al.* 2003; Yeh *et al.* 2005). It is thought that intracellular acidification causes a conformational change in the pore helix of TRPV5, subsequently facilitating channel closure induced by external protons (Yeh *et al.* 2005). External protons seem to reduce both open probability and unitary conductance of TRPV5, and a similar effect can be observed in endogenous TRPM2 channels measured in human neutrophils (Fig. 5). When increasing extracellular acidity from pH 7 to pH 5, single-channel activity not only subsides within 60 s in these cells, the open probability of the channel appears reduced and single channel conductance falls from 44 pS at pH 7 to 29 pS (Fig. 5). The latter effect is likely to be due to the permeation of protons themselves, causing the reduction in single channel currents, and accordingly is not observed when pH 6 is directly applied to the intracellular side of excised membrane patches in heterologously expressed TRPM2. Here, a rapid closure of TRPM2 can be observed (Fig. 4*A*), as revealed by the all-point histogram (Fig. 4*B*). The open channel current during both pH 7 (4–6 channels open) and pH 6 (4–0 channels open) remains around −5 pA at −80 mV. This corresponds to a single-channel conductance of 62 pS at −80 mV, as has been reported previously (Perraud *et al.* 2001). This is slightly higher than the slope conductance of inward currents observed for TRPM2 in human neutrophils (Lange *et al.* 2008), and may be due to differences in accessory proteins or channel subunits in these two cell systems.

The results of the present study have significant implications for the physiological and pathophysiological function of TRPM2 in that acidic pH environments will downregulate channel activity and Ca^{2+} transport of TRPM2. Extracellular acidosis significantly affects the immune response (Lardner, 2001). A number of studies have addressed pH effects on neutrophil activation and cytotoxicity. Early studies reported inhibitory effects of extracellular acidification on neutrophil function (Kellum *et al.* 2004). More recent experiments indicate a facilitation of fMLP-induced neutrophil activation partially due to increased H_2O_2 production during acidic conditions (Trevani *et al.* 1999). TRPM2 is known to be activated by H_2O_2 treatment (Hara *et al.* 2002; Perraud *et al.* 2005) and has been shown to be at least partially involved in fMLP-induced migration of mouse neutrophils (Yamamoto *et al.* 2008). Therefore, our data indicate that both the external and internal adjustments in acidity observed during physiological responses of neutrophils may provide a negative feedback mechanism that fine-tunes cellular processes involving TRPM2.

A further significant physiological context is provided by the recent demonstration that TRPM2 is not only present in the plasma membrane, but also localized in lysosomal compartments (Lange *et al.* 2009), which are highly acidic with pH values of about 4 to 5. Here, TRPM2 can serve as a Ca^{2+} release channel and the concomitant flux of protons may serve as a negative feedback regulator to limit Ca^{2+} release. However, during

episodes of increased lysosomal pH, TRPM2 activity may be enhanced and augment Ca^{2+} release, possibly contributing to lysosomal events in support of apoptosis (Lange *et al.* 2009).

References

Beck A, Kolisek M, Bagley LA, Fleig A & Penner R (2006). Nicotinic acid adenine dinucleotide phosphate and cyclic ADP-ribose regulate TRPM2 channels in T lymphocytes. *FASEB J* **20**, 962–964.

Csanady L & Torocsik B (2009). Four Ca^{2+} ions activate TRPM2 channels by binding in deep crevices near the pore but intracellularly of the gate. *J Gen Physiol* **133**, 189–203.

Du J, Xie J & Yue L (2009). Modulation of TRPM2 by acidic pH and the underlying mechanisms for pH sensitivity. *J Gen Physiol* **134**, 471–488.

Fang JS, Gillies RD & Gatenby RA (2008). Adaptation to hypoxia and acidosis in carcinogenesis and tumor progression. *Semin Cancer Biol* **18**, 330–337.

Hara Y, Wakamori M, Ishii M, Maeno E, Nishida M, Yoshida T, Yamada H, Shimizu S, Mori E, Kudoh J, Shimizu N, Kurose H, Okada Y, Imoto K & Mori Y (2002). LTRPC2 Ca^{2+}-permeable channel activated by changes in redox status confers susceptibility to cell death. *Mol Cell* **9**, 163–173.

Isaev NK, Stelmashook EV, Plotnikov EY, Khryapenkova TG, Lozier ER, Doludin YV, Silachev DN & Zorov DB (2008). Role of acidosis, NMDA receptors, and acid-sensitive ion channel 1a (ASIC1a) in neuronal death induced by ischemia. *Biochemistry (Mosc)* **73**, 1171–1175.

Jiang J, Li M & Yue L (2005). Potentiation of TRPM7 inward currents by protons. *J Gen Physiol* **126**, 137–150.

Jordt SE, Tominaga M & Julius D (2000). Acid potentiation of the capsaicin receptor determined by a key extracellular site. *Proc Natl Acad Sci U S A* **97**, 8134–8139.

Kellum JA, Song M & Li J (2004). Science review: extracellular acidosis and the immune response: clinical and physiologic implications. *Crit Care* **8**, 331–336.

Kolisek M, Beck A, Fleig A & Penner R (2005). Cyclic ADP-ribose and hydrogen peroxide synergize with ADP-ribose in the activation of TRPM2 channels. *Mol Cell* **18**, 61–69.

Lambert S & Oberwinkler J (2005). Characterization of a proton-activated, outwardly rectifying anion channel. *J Physiol* **567**, 191–213.

Lange I, Penner R, Fleig A & Beck A (2008). Synergistic regulation of endogenous TRPM2 channels by adenine dinucleotides in primary human neutrophils. *Cell Calcium*.

Lange I, Yamamoto S, Partida-Sanchez S, Mori Y, Fleig A & Penner R (2009). TRPM2 functions as a lysosomal Ca^{2+}-release channel in beta cells. *Sci Signal* **2**, ra23.

Lardner A (2001). The effects of extracellular pH on immune function. *J Leukoc Biol* **69**, 522–530.

Li M, Du J, Jiang J, Ratzan W, Su LT, Runnels LW & Yue L (2007). Molecular determinants of Mg^{2+} and Ca^{2+} permeability and pH sensitivity in TRPM6 and TRPM7. *J Biol Chem* **282**, 25817–25830.

Lis A, Peinelt C, Beck A, Parvez S, Monteilh-Zoller M, Fleig A & Penner R (2007). CRACM1, CRACM2, and CRACM3 are store-operated Ca^{2+} channels with distinct functional properties. *Curr Biol* **17**, 794–800.

Liu D, Zhang Z & Liman ER (2005). Extracellular acid block and acid-enhanced inactivation of the Ca^{2+}-activated cation channel TRPM5 involve residues in the S3-S4 and S5-S6 extracellular domains. *J Biol Chem* **280**, 20691–20699.

McHugh D, Flemming R, Xu SZ, Perraud AL & Beech DJ (2003). Critical intracellular Ca^{2+} dependence of transient receptor potential melastatin 2 (TRPM2) cation channel activation. *J Biol Chem* **278**, 11002–11006.

McMahon SB & Jones NG (2004). Plasticity of pain signalling: role of neurotrophic factors exemplified by acid-induced pain. *J Neurobiol* **61**, 72–87.

Naves LA & McCleskey EW (2005). An acid-sensing ion channel that detects ischemic pain. *Braz J Med Biol Res* **38**, 1561–1569.

Nobles M, Higgins CF & Sardini A (2004). Extracellular acidification elicits a chloride current that shares characteristics with $I_{Cl(swell)}$. *Am J Physiol Cell Physiol* **287**, C1426–1435.

Perraud AL, Fleig A, Dunn CA, Bagley LA, Launay P, Schmitz C, Stokes AJ, Zhu Q, Bessman MJ, Penner R, Kinet JP & Scharenberg AM (2001). ADP-ribose gating of the calcium-permeable LTRPC2 channel revealed by Nudix motif homology. *Nature* **411**, 595–599.

Perraud AL, Takanishi CL, Shen B, Kang S, Smith MK, Schmitz C, Knowles HM, Ferraris D, Li W, Zhang J, Stoddard BL & Scharenberg AM (2005). Accumulation of free ADP-ribose from mitochondria mediates oxidative stress-induced gating of TRPM2 cation channels. *J Biol Chem* **280**, 6138–6148.

Pingle SC, Matta JA & Ahern GP (2007). Capsaicin receptor: TRPV1 a promiscuous TRP channel. *Handb Exp Pharmacol* **179**, 155–171.

Sano Y, Inamura K, Miyake A, Mochizuki S, Yokoi H, Matsushime H & Furuichi K (2001). Immunocyte Ca^{2+} influx system mediated by LTRPC2. *Science* **293**, 1327–1330.

Shimada S, Ueda T, Ishida Y, Yamamoto T & Ugawa S (2006). Acid-sensing ion channels in taste buds. *Arch Histol Cytol* **69**, 227–231.

Starkus J, Beck A, Fleig A & Penner R (2007). Regulation of TRPM2 by extra- and intracellular calcium. *J Gen Physiol* **130**, 427–440.

Tong Q, Zhang W, Conrad K, Mostoller K, Cheung JY, Peterson BZ & Miller BA (2006). Regulation of the transient receptor potential channel TRPM2 by the Ca^{2+} sensor calmodulin. *J Biol Chem* **281**, 9076–9085.

Trevani AS, Andonegui G, Giordano M, Lopez DH, Gamberale R, Minucci F & Geffner JR (1999). Extracellular acidification induces human neutrophil activation. *J Immunol* **162**, 4849–4857.

Vennekens R, Prenen J, Hoenderop JG, Bindels RJ, Droogmans G & Nilius B (2001). Modulation of the epithelial Ca^{2+} channel ECaC by extracellular pH. *Pflugers Arch* **442**, 237–242.

Xiong ZG, Pignataro G, Li M, Chang SY & Simon RP (2008). Acid-sensing ion channels (ASICs) as pharmacological targets for neurodegenerative diseases. *Curr Opin Pharmacol* **8**, 25–32.

Yamamoto S, Shimizu S, Kiyonaka S, Takahashi N, Wajima T, Hara Y, Negoro T, Hiroi T, Kiuchi Y, Okada T, Kaneko S, Lange I, Fleig A, Penner R, Nishi M, Takeshima H & Mori Y (2008). TRPM2-mediated Ca^{2+} influx induces chemokine production in monocytes that aggravates inflammatory neutrophil infiltration. *Nat Med* **14**, 738–747.

Yeh BI, Kim YK, Jabbar W & Huang CL (2005). Conformational changes of pore helix coupled to gating of TRPV5 by protons. *EMBO J* **24**, 3224–3234.

Yeh BI, Sun TJ, Lee JZ, Chen HH & Huang CL (2003). Mechanism and molecular determinant for regulation of rabbit transient receptor potential type 5 (TRPV5) channel by extracellular pH. *J Biol Chem* **278**, 51044–51052.

Author contributions

J.G.S. and A.F. conducted experiments and analysed data. J.G.S., A.F. and R.P. designed the project, interpreted the data and wrote the paper. The work was done at the Queens Medical Center in the Laboratory of Cellular and Molecular Signals. All authors have approved the final version.

Acknowledgements

We thank Stephanie Johne for excellent technical support. This work was supported by the Ingeborg v.F. McKee fund of the Hawaii Community Foundation Grant No. 09ADVC-44268 (J.G.S.) and NIH grant R01-GM063954 (R.P.).